

Graphite thin films as a high-performance thermal interface material

Mutsuaki Murakami^{a*}, Atsushi Tatami^a, and Masamitsu Tachibana^a

^a Material Solutions New Research Engine, KANEKA Corporation, Torikai-Nishi 5-1-1 Settsu Osaka, 566-0072, Japan.

*Corresponding author. Mutsuaki Murakami

ABSTRACT: We report the characteristics of graphite thin films as a thermal interface material (TIM). These films are 0.14 to 30 μm thick with the basal (a–b) plane oriented in the film plane direction. In films the thermal resistance (TR) is not proportional to the film thickness but decreases at an accelerated rate as the thickness decreases. As a result, the TR reaches down to $0.067 \text{ K}\cdot\text{cm}^2\text{W}^{-1}$ (pressure $40 \text{ N}\cdot\text{cm}^{-2}$) when the graphite film is $0.39 \mu\text{m}$ thick. This phenomenon occurs because the TR at the interface between graphite and electrode (copper) decreases nonlinearly. The graphite film behaves like a flexible material (particularly, that are less than $2 \mu\text{m}$ thick) and corresponds to the surface irregularities of the electrode, so that the thermal bonding close to surface contact can be realized. Moreover, high thermal conductivity in the film direction also contributes to the reduction of interface TR. The graphite thin film TIMs below $2 \mu\text{m}$ thick are invaluable for their small TR value, excellent high durability, and low sensitivity of the TR to pressure. It can be applied in a wide range of applications as a means of effective heat dissipation such as in the fine portions of a semiconductor chip, a power semiconductor, or an LED. In addition, the new type three-layer TIM with grease on the surfaces of 2 to 30 μm thick graphite film is expected to have improved TR and durability that is superior to that of the conventional composite type TIM.

Index Terms: Thermal interface material, Graphite thin film, Thermal resistance, Interfacial thermal resistance, Durability, Thermal managements.

Date of Submission: 15-09-2019 Date of acceptance: 03-10-2019

I. INTRODUCTION

It is well known that heat generated by electronic devices with ever increasing power consumptions is a significant problem in electronic industry and the development of a means of efficient heat dissipation is indispensable for improving the heat transfer capabilities in electronics. [1-3]

Thermal interface material (TIM) is a very important component in thermal management technology. [4-6] TIM is inserted between a heat generating device (for example, a heat source) and a heat dissipating device (for example, a heat sink) and has a function of smoothly moving the generated heat. The TIM characteristic is expressed by a thermal resistance (TR) value, which is the sum of two interfacial TR ($R_{\text{interface}}$) and the bulk TR (R_{bulk}). The value of TR_{bulk} is proportional to the thickness of the TIM and inversely proportional to its thermal conductivity and measurement area. Therefore, the TR is not an inherent physical property of the material but a practical value. Typical TIMs include greases, low melting point metal foils, phase change sheets, and composite type materials. Silicon grease and low melting point metal TIM have excellent TR characteristics such as $0.07 \text{ K}\cdot\text{cm}^2\text{W}^{-1}$ for Indium (In) metal (Pressure: $6 \text{ N}\cdot\text{cm}^{-2}$) and $0.13\sim 2.0 \text{ K}\cdot\text{cm}^2\text{W}^{-1}$ for Silicon grease (Pressure: $10 \text{ N}\cdot\text{cm}^{-2}$). [5] However, these TIMs have a problem in thermal durability. For example, since the melting point of In metal is $160 \text{ }^\circ\text{C}$, it melts and flows in the solder reflow process ($260 \text{ }^\circ\text{C}$).

Composite type is the most important TIM in which the thermal conductivity is improved by adding fine highly thermally conductive fillers such as carbons, metals, or ceramics with the interfacial thermal resistance reduced with grease or flexible polymer. However, when the amount of filler is increased to realize high thermal conductivity the flexibility is lost, and the $R_{\text{interface}}$ increases. For this reason, the thermal conductivity of a typical composite type TIM was in the 1 to 100 $\text{W}\cdot\text{m}^{-1}\text{K}^{-1}$ range, but it was difficult to achieve a TR value less than 0.2 $\text{K}\cdot\text{cm}^2\text{W}^{-1}$. [7] Thermal stability of grease or polymer was also a problem. The degradation of composite type TIM characteristic not only appear as an increasing TR value, but also as the “pump out” or “bleed” phenomena. It is imperative to develop a new TIM that has low TR value, high heat stability, durability, and chemical stability. In recent years, the thermal properties of nanocarbon materials have drawn attention, and low TR composite type TIMs incorporating nanocarbon fillers such as graphene [7-14] or CNTs [15,16] have been reported. However, these fillers do not essentially solve the problems of a composite type TIM of insufficient heat resistance and deterioration. Studies were also conducted for use flexible graphite films of 130 μm to 3 mm thick as a TIM, but they were not attractive as TIM because their TR values exceeded over 1.0 $\text{K}\cdot\text{cm}^2\text{W}^{-1}$. [17, 18]

This report describes the TIM characteristics of graphite thin film from 0.14 to 30 μm thick unlike the conventional composite type TIMs or thick graphite films and proposes two new types of graphite TIMs.

II. EXPERIMENTAL

2-1. Materials

Graphite thin films were prepared by carbonization and subsequent graphitization using a pyromellitic dianhydride (PMDA)/ 4, 4'-oxydianiline (ODA) type polyimide (PI) film [19-21]. Carbonization of the PI film was performed in a nitrogen flow and the PI undergoes thermal decomposition between 500 $^{\circ}\text{C}$ to 600 $^{\circ}\text{C}$. The heat-treatment above 1000 $^{\circ}\text{C}$ was carried out in argon flow using a Tammann type furnace with the heating rate of 20 $^{\circ}\text{C}\cdot\text{min}^{-1}$. The highest treatment temperature (HTT) was 3000 $^{\circ}\text{C}$ and the sample was held at the HTT for 20 minutes. The obtained film thickness was measured using a cross-sectional SEM photograph.

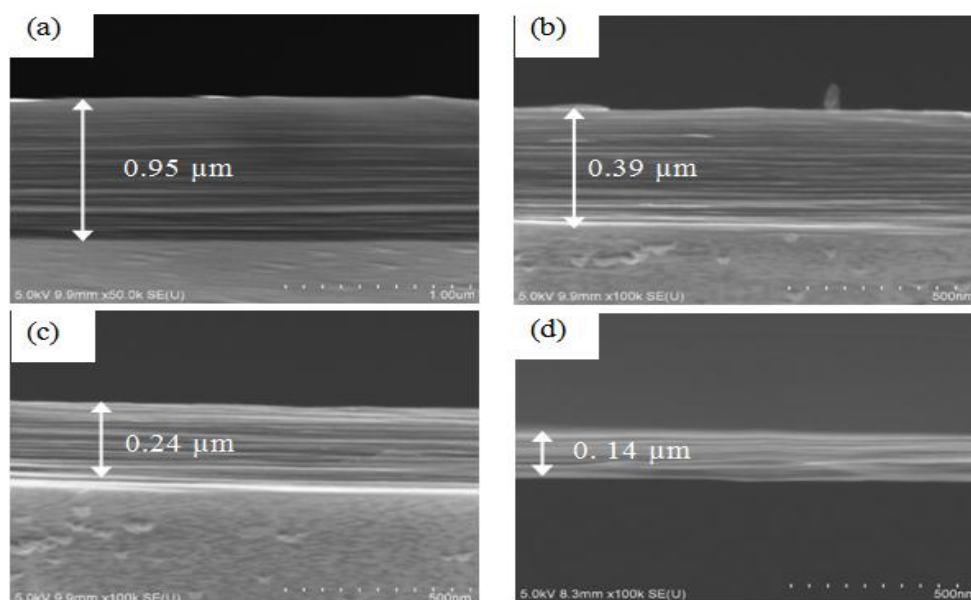


Fig. 1. SEM photographs of the cross-section of the graphite film with different thickness used in this paper.

Figure 1 shows an SEM photograph of the cross section of graphite films of different thickness. Layer structure was observed in the film plane direction in all samples. The variation in thickness within the film between 1 to 4 μm thick was within $\pm 0.1 \mu\text{m}$, and within $\pm 0.02 \mu\text{m}$ for films less than 1 μm thick.

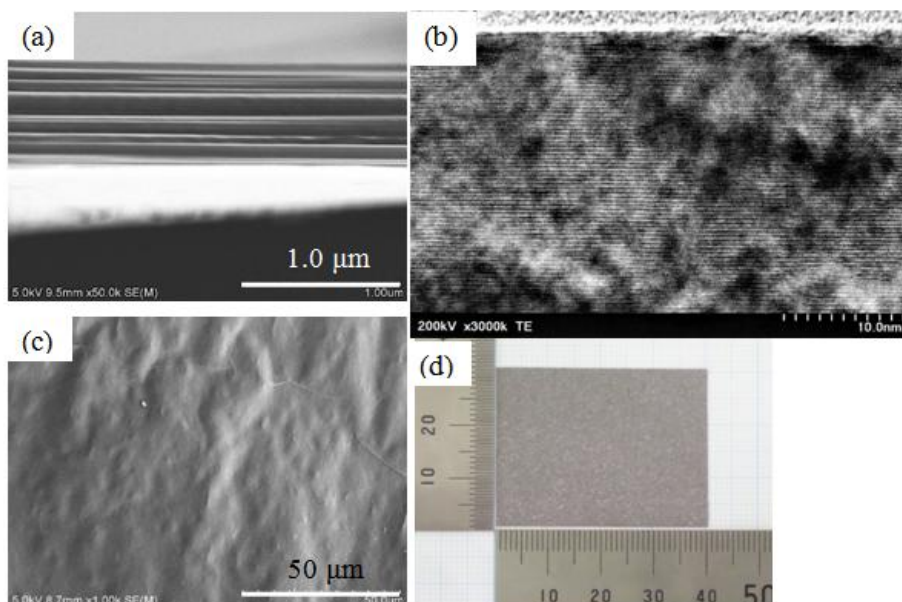


Fig.2. (a) Cross-sectional SEM photograph of the 0.67 μm thick film used in this paper. (b) Cross sectional photograph by TEM. (c) Typical film surface photograph by optical microscope. (d) Photograph of the film with an area of $4 \times 3 \text{cm}^2$.

Figure 2(a) and (b) show SEM and TEM photographs of the cross-section of the graphite film 0.67 μm thick. The cross-sectional SEM image (a) shows a striped structure, and the TEM image (b) shows a highly oriented layer structure. The latter interlayer distance was measured to be 0.336 nm, confirming that the structure was a well-oriented graphite layer (basal (a-b)) plane structure. From the results, it was proved that the striped structure of the film cross section corresponds to the graphite structure. Fig. 2(c) is an optical microscope photograph of the film surface. The surface of the all films with different thickness used in this paper was wrinkled and undulated to the same extent. Fig. (d) is a photograph of the film. Samples were made at least as large as the area of the measuring electrode. These films have high elastic constants and film with a thickness over 0.5 μm can be easily handled as free-standing films. [19]

2-2. Measurement of thermal diffusivity

The thermal diffusivities of the film surface direction of 1.0 to 30 μm thick measured by the periodic heating method (measurement frequency: 200 to 400 Hz) were 1.0 to $1.1 \times 10^3 \text{ m}^2 \cdot \text{s}^{-1}$. [22, 23] However, because this method has a large effect of heat dissipation, it was impossible to accurately measure of the samples less than 1.0 μm thick. The thermal diffusivity in the film thickness direction was also impossible because the measurement distance was too short.

The thermal diffusivity in the film thickness direction was measured by the laser flash method using 2 mm thick graphite block, produced by laminating and pressure firing a plurality of 1 μm thick sheets. [19, 22] The thermal diffusivity in the surface direction of the block was $1.2 \times 10^{-3} \text{ m}^2 \cdot \text{s}^{-1}$, and the film thickness direction was $4.6 \times 10^{-6} \text{ m}^2 \cdot \text{s}^{-1}$.

Although the latter value includes the interface TR between the plurality of graphite films, it is in agreement with the previously reported thermal diffusivity value in the interlayer direction of graphite. [24] When the density ($2.25 \times 10^3 \text{ kg} \cdot \text{m}^{-3}$) and the specific heat capacity ($740 \text{ J} \cdot \text{kg}^{-1} \cdot \text{K}^{-1}$) values of Highly Oriented Pyrolytic Graphite (HOPG) are used, the thermal conductivity in the film plane direction is $1998 \text{ W} \cdot \text{m}^{-1} \cdot \text{K}^{-1}$, and in the thickness direction is $7.6 \text{ W} \cdot \text{m}^{-1} \cdot \text{K}^{-1}$.

2-3. Measurement of thermal resistance

Measurement of TR was carried out using a precision TR measuring device manufactured by Hitachi Technology & Services Co., Ltd. Figure 3 shows the principle of the measurement. [25-27] The measurement was performed by sandwiching a graphite film between copper electrode rods having a square cross-sectional area of 1cm^2 and heating one electrode end (Fig. 3(a)). Thermocouples were embedded in the upper and lower electrode rods at regular intervals of 10 mm, and ΔT can be obtained from the difference in temperature gradient obtained

from the temperature at each point. The TR value (ΔT) is the total of the sample itself (R_{bulk}) and the two interface TR values ($R_{\text{interface}}$) between electrode and material. In a general TIM such as a composite type, the magnitude of $R_{\text{interface}}$ can be estimated by setting the thickness of TIM to zero, since the $R_{\text{interface}}$ is constant and R_{bulk} varies in proportion to the thickness of the material (Fig. 3(b)).

As already mentioned, the TR value is a practical value that changes according to the state of the electrode and the setting method of the sample, for example. [28] In order to minimize the influence of the electrodes, the electrode cylinder was made of pure copper, and after mechanical processing with a roughness of $0.2 \mu\text{m}$ the surface was further mirrorpolished. The actual center line calculation average roughness (Ra) was much smaller than 0.2 and estimated to be about 0.01 to 0.05 .

First, the thickness change of the graphite film by pressurization was estimated using the sample of $30.4 \pm 0.2 \mu\text{m}$ thick film. The electrode spacing in a pressurized state was measured, and the value was compared with the film thickness of the sample before pressing obtained by SEM measurement. When a pressure of $50 \text{ N}\cdot\text{cm}^{-2}$ was applied the average spacing value from 10 times measurements was $29.8 \mu\text{m}$. Therefore, it was estimated that the change in the film thickness due to pressurization in the range of 10 - $50 \text{ N}\cdot\text{cm}^{-2}$ was 2.6% at the maximum. From this result, we judged that the change in film thickness due to pressure was small, and we used the thickness obtained by TEM measurement for thermal resistance measurement. Due to the large gap measurement error, it was not possible to measure the change in film thickness due to the pressure of a film with a thickness of $4 \mu\text{m}$ or less.

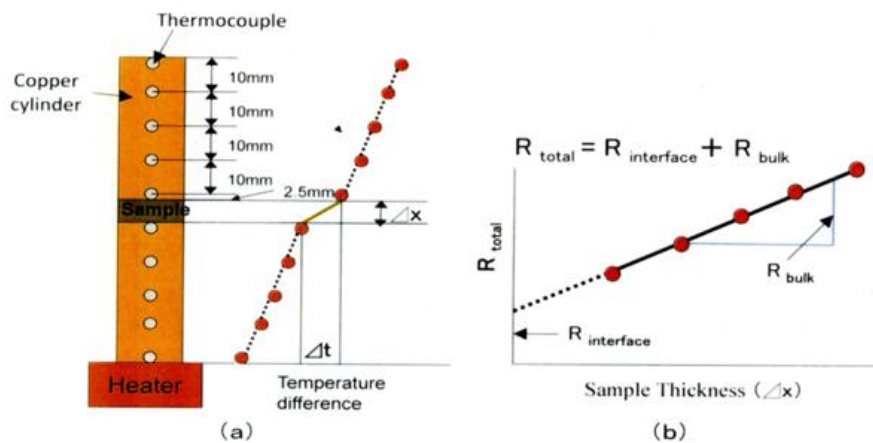


Fig. 3. (a) Principle of TR measurement. Steady-state method (Guarded Hot Plate method: GHP method). (b) Contents of the measured TR value. The value consists of bulk TR (R_{bulk}) and two interface TR ($R_{\text{interface}}$).

Power (W) was applied to obtain the interface temperature of $60 \text{ }^\circ\text{C}$, and then pressure from 10 to $50 \text{ N}\cdot\text{cm}^{-2}$ was applied. After the temperature became constant, the measurement was carried out 10 times and the average value was taken as the TR value. These conditions are determined by the ASTM D 50 570 method according to the American Society for Testing and Materials Standards. Since the TR value is influenced also by the adjustment state of the measuring apparatus, it was necessary to pay special attention to the measurement of a minute TR value. In order to check if the measuring apparatus adjustment is normal, the silicon grease (Shin-Etsu Chemical Co. Ltd, G747, thermal conductivity: $0.90 \text{ W}\cdot\text{m}^{-1}\text{K}^{-1}$) was coated on the electrode surface and the load of $40 \text{ N}\cdot\text{cm}^{-2}$ was applied. When the measured value was equal to $0.10 \text{ K}\cdot\text{cm}^2\text{W}^{-1}$, it was judged that the condition of the measuring instrument was normal. This procedure is a standard method for achieving the lowest TR in a thermal measurement apparatus using steady-state method. By these techniques, even in the measurement of small TR, the measurement error could be made within 10% .

III. RESULTS AND DISCUSSION

3-1. Relationship between TR and film thickness

The TR value when the electrodes are in direct contact (without TIM) was $1.35 \text{ K}\cdot\text{cm}^2\text{W}^{-1}$ and the value when a $30 \mu\text{m}$ thick graphite film is sandwiched was $0.54 \text{ K}\cdot\text{cm}^2\text{W}^{-1}$. Therefore, in principle, a film having a thickness of at least $30 \mu\text{m}$ or less functions as a TIM. Figure 4 shows the relationship between the film thickness (0.95 to $30 \mu\text{m}$) and the TR value. The line (a) is the relationship when the pressure is $10 \text{ N}\cdot\text{cm}^{-2}$ and (b) is $40 \text{ N}\cdot\text{cm}^{-2}$. In either case, TR value decreased sharply as the films became thinner, and there was no linear proportional relationship between the thickness and the TR. The value at a film thickness of $0.95 \mu\text{m}$ under $40 \text{ N}\cdot\text{cm}^{-2}$ was $0.12 \text{ K}\cdot\text{cm}^2\text{W}^{-1}$. Such relationship between thickness and TR is not known in conventional TIMs.

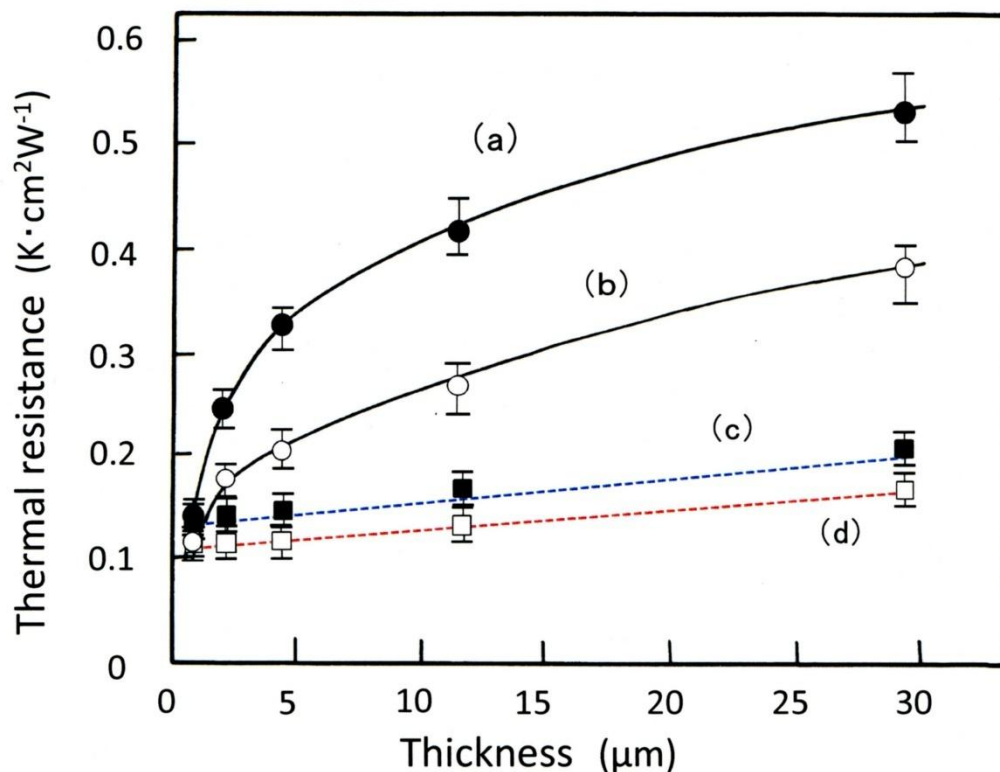


Fig.4. Thickness dependence of TR value of the graphite films from 30 to $0.95 \mu\text{m}$ thick. (a) under pressure of $10 \text{ N}\cdot\text{cm}^{-2}$, (b) under pressure of $40 \text{ N}\cdot\text{cm}^{-2}$.

The value when silicone grease coated electrodes were used, (c) under pressure of $10 \text{ N}\cdot\text{cm}^{-2}$, (d) under pressure of $40 \text{ N}\cdot\text{cm}^{-2}$.

The TR value was measured using an electrode coated with a small amount of silicone grease (G 747) on the surface. This is a method of making the $R_{\text{interface}}$ as small as possible and constant. Figure 4(c) and (d) show the relationship between the film thickness and TR, measured under a pressure of $10 \text{ N}\cdot\text{cm}^{-2}$ and $40 \text{ N}\cdot\text{cm}^{-2}$, respectively. The use of grease greatly reduced the TR particularly in the range of 2 to $30 \mu\text{m}$ thick film, and the relationship also changed to the linear dependence as the conventional composite type TIM. When the film thickness was extrapolated to thickness zero the estimated $R_{\text{interface}}$ value was $0.10 \text{ K}\cdot\text{cm}^2\text{W}^{-1}$ for $40 \text{ N}\cdot\text{cm}^{-2}$ pressure. This value was the same as the value when equipment adjustment is performed using only grease. For example, TR value of $30 \mu\text{m}$ thick graphite film is $0.165 \text{ K}\cdot\text{cm}^2\text{W}^{-1}$, so the R_{bulk} value is estimated to be $0.065 \text{ K}\cdot\text{cm}^2\text{W}^{-1}$ and it shows that 88% of the TR value ($0.53 \text{ K}\cdot\text{cm}^2\text{W}^{-1}$) of without grease is the $R_{\text{interface}}$.

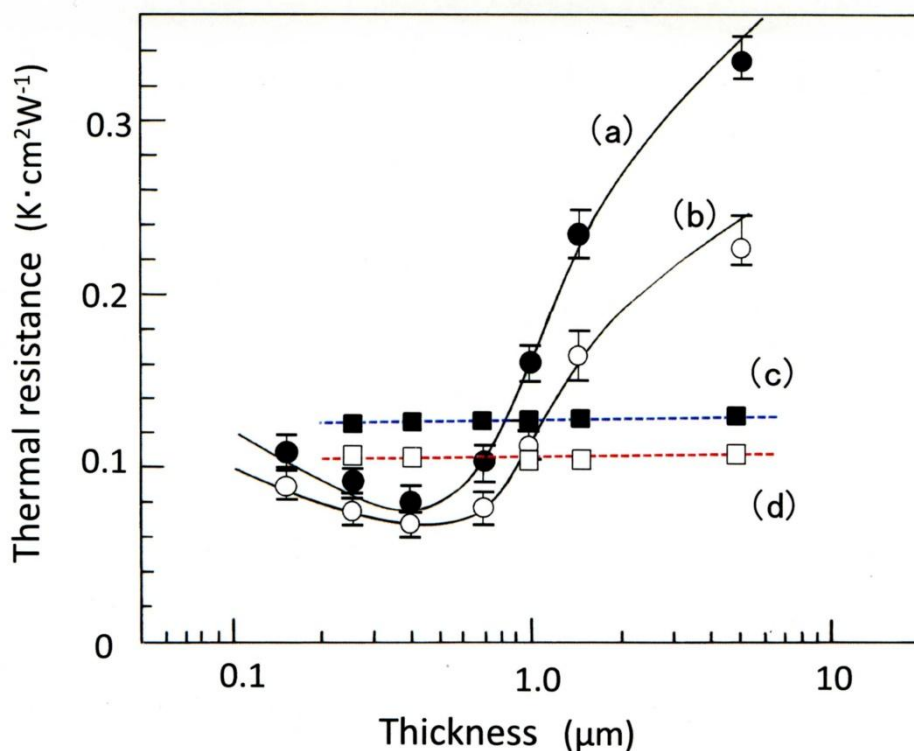


Fig. 5. Thickness dependence of TR values of the films from 4.8 to 014 μm thick, (a) under pressure of $10 \text{ N}\cdot\text{cm}^{-2}$, (b) under pressure of $40 \text{ N}\cdot\text{cm}^{-2}$. Thickness dependence of TR value when grease coated electrode was used, (c) under pressure of $10 \text{ N}\cdot\text{cm}^{-2}$, (d) under pressure of $40 \text{ N}\cdot\text{cm}^{-2}$.

Figure 5 shows the relationship between the TR value and film thickness below $4.8 \mu\text{m}$. Fig. 5(a) and (b) show the characteristics under pressure of $10 \text{ N}\cdot\text{cm}^{-2}$ and $40 \text{ N}\cdot\text{cm}^{-2}$, respectively, and (c) and (d) show the characteristics when using silicon grease coated electrodes. The TR value is almost constant when using a coated electrode, indicating that the R_{bulk} value of a graphite film with a thickness of less than $4.8 \mu\text{m}$ is so small that it has little effect on the measured TIM characteristics.

The TR values of the graphite films from 0.67 to $0.14 \mu\text{m}$ thick were ranging from 0.067 to $0.10 \text{ K}\cdot\text{cm}^2\text{W}^{-1}$ (pressure $40 \text{ N}\cdot\text{cm}^{-2}$). In particular, the value of $0.39 \mu\text{m}$ thick was $0.067 \text{ K}\cdot\text{cm}^2\text{W}^{-1}$, resulting in extremely small TR values. The TR values were smaller than the value achieved with only silicon greases or graphite films using silicon coated electrodes, meaning that the $R_{\text{interface}}$ value between copper and graphite was smaller than between copper and fluid greases.

3-2. Thermal boundary conductance of the interface

The influence of the surface conditions on the TR value decrease was considered to be small, since the surface wrinkling and undulation of all films used were similar. On the other hand, graphite thin films are flexible, and their flexibility increases with thinner films. Unlike the surface conditions, increase in the flexibility is believed to have a major impact on the decrease in the TR value. The films less than $1 \mu\text{m}$ thick had a sufficient flexibility to substantially fill the asperities on the surface of the electrode, and the thickness of $0.39 \mu\text{m}$ may be optimal. Increase in TR of the films of 0.14 and $0.24 \mu\text{m}$ thick were likely because the thickness may be insufficient to fill the irregularities of the electrode surface or a gap caused by slight deviations from perfect parallelism of the electrodes. To identify the reason, it is necessary to compare with the more detailed structures of the electrode, but it was not possible to identify the reason.

However, it is unclear whether the increase in contact area due to the increase in film flexibility is sufficient to account for the non-linear decrease in the TR value. Most of the thermal conductivity of a graphite is due to acoustic phonon oscillations. [29-31] The acoustic mismatch model (AMM) and the diffuse mismatch model (DMM) have been used to calculate the

thermal boundary conductance of interfaces. The AMM assumes a geometrically perfect interface and phonon transport across it is entirely elastic, treating phonons as waves in a continuum, and the DMM assumes scattering at the interface is diffusive, which is accurate for interfaces with characteristic roughness. In these calculations, the distance of the interface is an important factor and the phonon dispersion relationship is usually approximated by a linear relationship (Debye approximation). [32,33] In order to understand the nonlinear TR properties of the graphite thin film and the metal interface, it may be necessary to take into account any specific interactions between the metal electrode and graphite. There are several reports on specific interactions regarding heat conduction at the contact interface between graphene and another solid. Abnormal thermal conductivity has been measured between graphene and Cu [34], SiO₂ [35, 36], SiC [37], GaN [37], and BN [38] suggesting strong interaction at the interface. Such strong interactions should affect the distance and contribute to the non-linear decrease of the thermal boundary conductance value.

In general, vibrations are transmitted through a macroscopic system, and the subsequent heat conduction is described by the Fourier law. However, phonons are known to ballistically diffuse if the typical length of the system is shorter than the phonon mean free path. In the case of crossovers where these lengths are comparable, there is quasi-ballistic phonon conduction where there is ballistic and Fourier type phonon behavior. [39-41] Even in such a scenario, phonon scattering inevitably occurs at an actual solid interface and is influenced by the state of the contact interface, so it is necessary to consider the heat conduction mechanism including the interface as one system. However, the theoretical framework for the quasi-ballistic heat transfer mechanism in the thickness direction of the graphite thin film has not been determined [42], and the R_{bulk} of less than 1 μm thick was much smaller than the observed TR value. Therefore, it is difficult to discuss the possibility of quasi-ballistic heat transfer mechanism from the measurement results described in this paper.

3-3. Bonding state and the heat flow

Figure 6(a) depicts the state of the contact between electrodes in the absence of a TIM. Due to the surface irregularity, a low thermal conductive air layer ($0.02 \text{ W}\cdot\text{m}^{-1}\cdot\text{K}^{-1}$) is present between the electrodes. The $R_{\text{interface}}$ increases because the heat flow (red arrows) is transmitted only through the limited contact points. Fig. 6(b) shows the bonding state when a grease is used. The grease flows by pressure and fills the concave portion of the interface so that the air layer is removed to complete the surface contact and contribute to the low $R_{\text{interface}}$ characteristics. However, heat flow tends to concentrate at the points where the distance between the electrodes is relatively narrow, resulting in uneven heat flow. A similar non-uniform heat flow also occurs to some extent in composite type TIMs, which causes bleeding and pump out phenomena.

Figure 6(c) shows the contact state of the graphite thin film sandwiched between the electrodes. The distance between electrodes is larger than that in (b), but the thermal conductivity in the thickness direction ($7.6 \text{ W}\cdot\text{m}^{-1}\cdot\text{K}^{-1}$) is larger than the grease ($0.9 \text{ W}\cdot\text{m}^{-1}\cdot\text{K}^{-1}$) and the value in the film direction is very high ($1998 \text{ W}\cdot\text{m}^{-1}\cdot\text{K}^{-1}$). Therefore, the heat flowing from the high temperature side rapidly diffuses in the graphite film and flows out from the large number of contacts on the film to the cooling electrode side, which indicates that the high thermal conductivity in the film direction also contributes to the realization of low TR value. [43, 44]

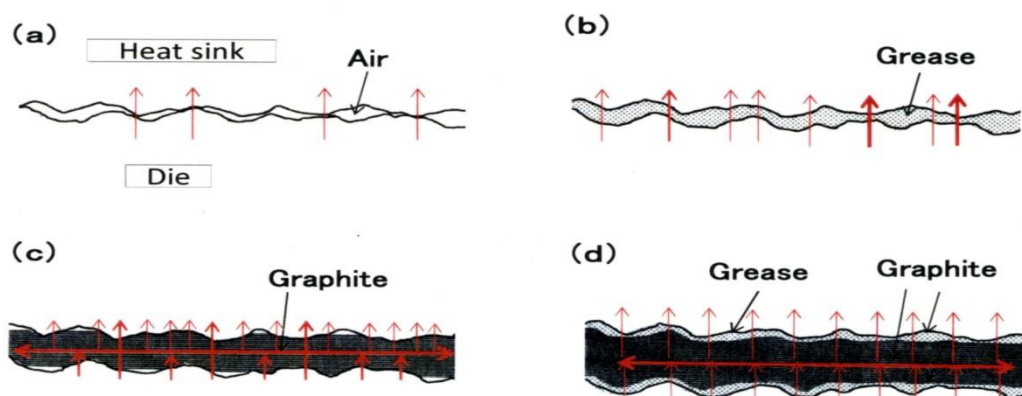


Fig.6. Contact state and heat flow mechanism between die and heat sink.
 (a) Direct contact of electrodes (without TIM). (b) Silicon grease type TIM.
 (c) Graphite thin film type TIM. (d) Grease coated graphite thin film type TIM.

Fig.6(d) shows the thermal bonding when grease is exists between the electrode and graphite film. Although, the TR value is the same as that of grease alone, the heat concentration can be avoided by high thermal conduction in the film direction. The durability is thus improved, and this property distinguishes this TIM from the conventional composite type TIMs.

3-4. Effect of electrode surface roughness

Although the graphite thin film TIM is extremely effective for an electrode with a small surface roughness as used in measuring apparatus, the influence of the surface roughness is not well understood. We prepared two kinds of copper electrodes (A, B) having different interfacial roughness, and measured the TR of four graphite films (thickness: 5.0, 1.8, 0.96, 0.42 μm) and grease coated graphite film (3.6 μm).

The measurement results were shown in Table 1. The error of the measured TR values in this experiment was ±0.03 K·cm²W⁻¹. Results were summarized as follows. (1) The reducing behavior of TR was greater in thinner graphite films. (2) The pressure dependence of TR was small, and the low TR values have been achieved even with small loads. (3) Graphite thin films of about 2.0 μm thick (at least less than 1.8 μm) were TIMs that can be used for electrodes with Ra less than 0.2. (4) But these effects ((1), (2)) were small for the electrode B having a large surface roughness. (5) On the other hand, grease coated graphite TIM was hardly affected by electrode roughness and had excellent TR characteristics for either two electrodes.

TABLE 1 Thermal resistance value of TIMs when electrodes with different surface roughness A (Ra:0.20 μm, Rz:2.60 μm) and B (Ra:0.27 μm, Rz:3.36 μm) were used.

Electrode	Graphite Thickness (μm)	Thermal resistance (K·cm ² W ⁻¹)			Pressure Dependency (10N/40N)
		10 N·cm ⁻²	20 N·cm ⁻²	40 N·cm ⁻²	
A	Blank	0.54	0.41	0.31	1.74
	5.0	0.40	0.33	0.25	1.60
	1.8	0.20	0.18	0.15	1.33
	0.95	0.16	* ² —	0.13	1.23
	0.42	0.12	* ² —	0.10	1.20
	*13.6	0.13	0.12	0.11	1.18
B	Blank	0.44	0.37	0.26	1.69
	5.0	0.40	0.32	0.26	1.54
	1.8	0.30	* ² —	0.24	1.25
	0.95	0.28	* ² —	0.23	1.22
	0.42	0.21	* ² —	0.17	1.24
	*13.6	0.14	0.12	0.11	1.27

*¹Grease coated graphite film. *²Not measured.

3-5. Characteristic comparison with commercial TIMs

Four representative types of commercially available high-performance TIMs were obtained, and their properties compared to those of the graphite film TIMs. Selections were, (a) Silver paste type TIM (Akasa Corp., AK-450-5G, thermal conductivity: $9.2 \text{ W}\cdot\text{m}^{-1}\text{K}^{-1}$), (b) Phase change type TIM (Ainex Co. Ltd., HT-08A, $3.0 \text{ W}\cdot\text{m}^{-1}\text{K}^{-1}$), (c) Graphite filler composite type TIM (Shinwa Sangyo Co. Ltd., ICG30, $35 \text{ W}\cdot\text{m}^{-1}\text{K}^{-1}$), (d) Vertically oriented graphite composite type TIM (Wide work Corp., WW-90VG, $90 \text{ W}\cdot\text{m}^{-1}\text{K}^{-1}$). These are all high performance TIMs that show a low thermal resistance of less than $0.3 \text{ K}\cdot\text{cm}^2\text{W}^{-1}$ under a pressure of $10 \text{ N}\cdot\text{cm}^{-2}$ in our measurements

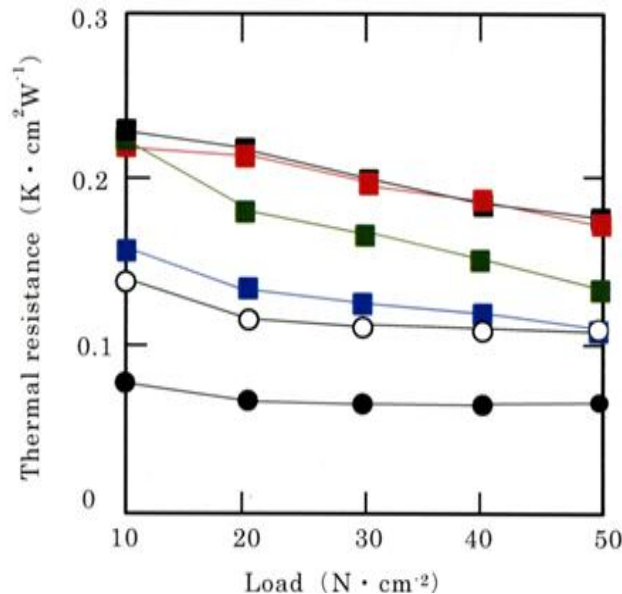


Fig. 7. Pressure dependence of TR values of various TIMs.

- : Graphite thin film ($0.39 \mu\text{m}$), ○: Grease coated Graphite film ($3.6 \mu\text{m}$),
- : Silver paste, ■: Phase change type, ■: Graphite composite type,
- : Vertically oriented graphite composite type.

Figure 7 shows the pressure dependence of TR of these TIMs as compared to graphite TIM ($0.39 \mu\text{m}$) and graphite film ($3.6 \mu\text{m}$) TIM coated with silicone grease. The choice of commercial TIMs is random and this data does not imply that it is the highest quality of each type of TIM, but the two graphite TIMs showed better TR properties than either TIMs. Furthermore, it was found that a graphite film of $0.39 \mu\text{m}$ thick has a significantly low TR dependence on pressure. The values at the pressure of $10 \text{ N}\cdot\text{cm}^{-2}$ ($0.076 \text{ K}\cdot\text{cm}^2\text{W}^{-1}$) and $40 \text{ N}\cdot\text{cm}^{-2}$ ($0.067 \text{ K}\cdot\text{cm}^2\text{W}^{-1}$) differ only by 1.13 times. For several layers of graphene, it is expected that the TR will decrease by calculation using the Green function under large pressure [45], but it is considered that the R_{bulk} value does not change under a small pressure like this measurement. The small effect of pressure on the $R_{\text{interface}}$ can be considered to indicate that the graphite thin film has already achieved a connection close to the surface contact. This dependence demonstrates that the substantial pressurization (tightening) is not required to achieve low TR characteristics and is a practically important characteristic.

3-6. Proposal of two types of TIMs

Here, we propose two types of TIMs. One is the graphite film TIM of 0.2 to $2 \mu\text{m}$ thick, which can be handled by hand or tweezers. [19] The graphite material has an excellent durability and chemical stability, and the heat resistance of the film is $600 \text{ }^\circ\text{C}$ in air. Also, graphite is used as a solid lubricant and the film is flexible enough to accommodate thermal expansion of the electrode, since the basal plane is oriented in the film surface direction. In fact, the Cu/graphite thin film/Cu junction was heated at $300 \text{ }^\circ\text{C}$ for 30 hours in air, but its TR value did not change at all. This characteristic is extremely useful for TIM in high temperature environments where grease or polymers cannot be used like in the fine portions of a semiconductor chip, a power semiconductor or an LED. The graphite thin film TIM can be expected to be a new type of TIM

that meeting the stringent requirements for heat dissipation in the electronics field.

The second is a three-layer type TIM in which grease or flexible polymer was applied to both surfaces of the graphite film having a thickness of about 2 to 30 μm . This type of TIM not only has excellent TR characteristics, but also uniformly transport the heat due to the high thermal conductivity in the plane direction of the graphite film. Therefore, it is characterized in that its durability is improved and "pump-out" and "bleed" phenomena are less likely to occur. It is a high-performance TIM that improves the shortcomings of the conventional composite type TIMs.

IV. CONCLUSION

Graphite thin film has excellent properties as a TIM. The $R_{\text{interface}}$ of graphite thin films with 0.2 to 2 μm thick were very small resulting in TIM having excellent TR characteristics and extremely high durability. The TIM can be used in a wide range of applications as a means of effective heat dissipation. Graphite thin films of 2 to 30 μm thick provided with a flexible layer on the surface are a new structure TIM with improved TR characteristics and durability of the conventional composite TIM.

Conflict of interest

We declare that we have no financial and personal relationship with other people or organization that can inappropriately influence our work.

ACKNOWLEDGMENT

This paper is based on results obtained from a project commissioned by the New Energy and Industrial Technology Development Organization of Japan (NEDO). We appreciate Mrs. Miyuki Nakai who is an assistant in experiments and measurements.

REFERENCES

- [1]. International Technology Roadmap for Semiconductors: ITRS Reports, <http://www.itrs.net/reports.html>. Google Scholar
- [2]. A. L. Moore, and Li. Shi, "Emerging challenges and materials for thermal management of electronics," *Materials Today* 17(4), 163-174 (2014).
- [3]. J. Wei, "Challenges in Cooling Design of CPU Packages for high-performance servers," *Heat Transfer Engineering*, 29(2), 178-187 (2008)
- [4]. R. Prasher, "Thermal Interface Materials: Historical Perspective, Status, and Future Directions," *Proc IEEE* 2006, 94 1571-1585.
- [5]. F. Sarvar, D. C. Whalley, and P. P. Conway, "Thermal interface materials-a review of the state of the art," *Proc. Electron. Syst. Integr. Technol. Conf. (IEEE 1-4244-0553)* 2, 1292-1302 (2006).
- [6]. K. M. Razeeb, E. Dalton, G. L. W. Cross, and A. J. Robinson, "Present and future interface materials for electronic devices," *International Materials Reviews*, 63(1), 1-21 (2017)
- [7]. K. M. F. Shahil and A. A. Barandin, "Graphene-multilayer graphene nanocomposite as highly efficient thermal interface materials," *Nano Lett.* 12, 861-867 (2012).
- [8]. S. I. Ghosh, C. D. Teweldebrhan, F. P. Pokatillov, D. L. Nika, A. A. Balandin, W. Bao, F. Miao, and C. N. Lau, "Extremely high thermal conductivity of graphene: Prospects for thermal management applications in nanoelectronic circuits," *Appl. Phys. Lett.* 92, 151911-151911-3 (2008).
- [9]. Z. Gao, Y. Zhang, Y. Fu, M. M. F. Yuen, and J. Liu, "Thermal chemical vapor deposition grown graphene heat spreader for thermal management of hot spots," *Carbon* 61, 342-348 (2013).
- [10]. B. Tang, H. Goouxin, H. Gao, and L. Hai, "Application of graphene as filler to improve thermal transport property of epoxy resin for thermal interface material," *Inter. J. Heat and Mass Transfer* 85, 420 (2015).
- [11]. Q. Li, Y. Guo, W. Li, S. Qiu, C. Zhu, X. Wei, M. Chen, C. Liu, S. Liao, Y. Gong, A. K. Mishra, and L. Liu, "Ultra-high thermal conductivity of assembled aligned multilayer graphene/epoxy composite," *Chem. Mater.* 26, 4459-4465 (2014).
- [12]. K. M. F. Shahil and A. A. Balandin, "Thermal properties of graphene and multilayer graphene: Application in thermal interface materials," *Solid State Comm.* 152, 1331-1340 (2012).
- [13]. A. S. Dmitriev and A. R. Valeev, "Graphene nanocomposites as thermal interface materials for cooling energy device," *J. Phys. Conf. Series* 891, 012359 (2017).
- [14]. W. Park, Y. Guo, X. Li, J. Hu, L. Liu, X. Ruan, and Y. P. J. Chen, "High-performance thermal interface material based on few-layer graphene composite," *Phys. Chem. C* 119, 26753-26759 (2015).
- [15]. G. Yujun, L. Zhongliang, Z. Guangmeng, and L. Yanxia, "Effect of multi-walled carbon nanotubes addition on thermal properties of thermal grease," *Inter. J. Heat and Mass Transfer* 74, 358-367 (2014).
- [16]. K. Zhang, Y. Chai, M. M. F. Yuen, D. G. W. Xiao, and P. C. H. Chan, "Carbon nanotube thermal interface material for high-brightness light-emitting-diode cooling," *Nanotech.* 19, 215706 (2008).
- [17]. M. Smalc, J. Norley, R. A. Reynolds, R. Pachuta, and D. W. Krassowski, "Advanced Thermal Interface materials using Natural Graphite," *Proc. International Electronic Packaging Technical Conference*, July 06-11, 2003 253-261.
- [18]. E. E. Marotta, "Thermal joint conductance for flexible graphite materials," *Analytical and experimental study*,

- IEEE Transactions on Component and Packaging Technologies, 28(1) 102-110 (2005).
- [19]. M. Murakami, A. Tatami, and M. Tachibana, "Fabrication of high quality and large area graphite thin films by pyrolysis and graphitization of polyimides," *Carbon* 145, 23-30 (2019)
- [20]. M. Murakami, N. Nishiki, N. Nakamura, J. Ehara, T. Kouzaki, K. Watanabe, T. Hoshi, and S. Yoshimura, "High-quality and highly oriented graphite block from poly-condensation polymer films," *Carbon* 30, 255-262 (1992).
- [21]. M. Inagaki, T. Takeichi, Y. Hishiyama, and A. Oberin, "High quality graphite films produced from aromatic polyimides," *Chemistry and Physics of Carbon* 26, 245-333 (1999), Marcel Dekker, Inc.
- [22]. A. Tatami, M. Tachibana, T. Yagi, M. Akoshima, and M. Murakami, Proceedings of the 15th Inter. Heat Transfer Conference, IHTC-15, August 10-15 (2014) Kyoto, Japan.
- [23]. A. Tatami, M. Tachibana, T. Yagi, and M. Murakami, AIP Conference Proceeding 1962, 030005 (2018).
- [24]. A. W. Moore, "Highly Oriented Pyrolytic Graphite," *Chemistry and Physics of Carbon*, Vol. 11, 70 (1973), Marcel Dekker, Inc.
- [25]. J.-J. Park and M. Taya, "Design of Thermal Interface material with High Thermal Conductivity and Measurement Apparatus," *J. Electronic Packaging*, Vol. 128m 46-52, (2006)
- [26]. ASTM D5470-06 Standard, "Test Method for Thermal Transmission Properties of Thermally Conductive Electrical Insulation Materials", DOI: 10.1520/D5470-06, www.astm.org
- [27]. R. Kempers, P. Kolodner, A. Lyons, and A. J. Robinson, "A high-precision apparatus for the characterization of thermal interface materials," *Review of Scientific Instruments* 80, 095111 (2009)
- [28]. C. J. M. Lasance, C. T. Murray, D. L. Saums, and M. Rencz, "Challenges in thermal interface material testing," *The 22nd Annual IEEE SEMI-THERM Symposium*, 14-16 March 2006, Dallas, TX, USA, pp. 42-49.
- [29]. P. G. Klemens and D. F. Pedraza, "Thermal conductivity of graphite in the basal plane," *Carbon* 32(4), 735-741 (1994).
- [30]. P. G. Klemens, "Theory of the a-plane thermal conductivity of graphite," *J. Wide Bandgap Materials* 7(4), 332-339 (2000).
- [31]. A. Alofi and G. P. Srivastava, "Thermal conductivity of graphene and graphite," *Phys. Rev. B* 87, 115421 (2013).
- [32]. E. T. Swartz and R. O. Pohl, "Thermal boundary resistance," *Reviews of Modern Physics* 61, 3, 605-668 (1989)
- [33]. D. G. Cahill, P. V. Braun, G. C. Chen, D. R. Clarke, S. Fan, K. E. Goodson, P. Keblinski, W. P. King, G. D. Mahan, A. Majumdar, H. J. Maris, S. R. Phillpot, E. Pop, and L. Shi, "Nanoscale thermal transport. II. 2003-2012," *Applied Physics Rev.* 1, 011305-1-45 (2014)
- [34]. P. Goli, H. Ning, X. Li, C. Y. Lu, K. S. Novoselov, and A. A. Balandin, "Thermal properties of graphene-copper-graphene heterogeneous films," *Nano Lett.* 14(3), 1497-1503 (2014).
- [35]. W. Jang, Z. Chen, W. Bao, C. N. Lau, and C. Dames, "Thickness-dependent thermal conductivity of encased graphene and ultrathin graphite," *Nano Lett.* 10 (10), 3909-3913 (2010).
- [36]. Y. K. Koh, A. S. Lyons, M.-H. Base, B. Huang, V. E. Dorgan, V. E. Cahill, and E. Pop, "Role of remote interfacial phonon (RIP) scattering in heat transport across graphene/SiO₂ interface," *Nano Lett.* 16, 6014-6020 (2016).
- [37]. M. Hu and D. Poulikakos, "Graphene mediated thermal resistance reduction at strongly coupled interfaces," *J. Heat and Mass Transfer* 62, 205-213 (2013).
- [38]. R. Mao, B. D. Kong, K. W. Kim, T. Jayasekera, A. Calzolari, and M. B. Nardell, "Phonon engineering on nanostructures: Controlling interfacial thermal resistance in multilayer-graphene/dielectric heterojunction," *Appl. Phys. Lett.* 101, 113111 (2012).
- [39]. T. Yamamoto, S. Konabe, J. Shiomi, and S. Maruyama, "Crossover from ballistic to diffusive thermal transport in carbon nanotubes," *Appl. Phys. Express* 2, 095003 (2009).
- [40]. C. W. Chang, D. Okawa, H. Garcia, A. Majumdar, and A. Zetti, "Breakdown of Fourier's law in nanotube thermal conductor," *Phys. Rev. Lett.* 101, 075903 (2008).
- [41]. J. Shiomi and S. Maruyama, "Molecular dynamics of diffusive-ballistic heat conduction in single-walled carbon nanotubes," *Jpn. J. Appl. Phys.* 47, 2005-2009 (2008).
- [42]. I. Paulatto, F. Mauri, and M. Lazzeri, "Anharmonic properties from a generalized third-order ab initio approach: Theory and applications to graphite and graphene," *Phys. Rev. B* 87, 214303 (2013).
- [43]. Y. Ni, Y. Chalopin, and S. Vioz, "Few layers graphene based superlattices as efficient thermal insulators," *Appl. Phys. Lett.* 103, 141905 (2013)
- [44]. Y. Ni, Y. Chalopin, and S. Volz, "Significant thickness dependence of the thermal resistance between few-layer graphenes," *Appl. Phys. Lett.* 103, 061906 (2013).
- [45]. C. Liu, Z. Wei, W. Chen, K. Bi, J. Yang, and Y. Chen, Y., "Pressure effect on the thermal resistance of few-layer graphene," *Physics Letters A*, 380, 248-254 (2016).

Mutsuaki Murakami" Graphite thin films as a high-performance thermal interface material" *International Journal of Modern Engineering Research (IJMER)*, vol. 09, no. 5, 2019, pp 09-19